Novel Binding Modes and Hemilability in Atropisomeric Phosphino−Amino Palladium Complexes

J. W. Faller* and Nikos Sarantopoulos

Department of Chemistry, Yale University, 225 Prospect Street, New Haven, Connecticut 06520

Received December 4, 2003

Two new allyl complexes of palladium bearing the atropisomeric ligands 2-(diphenylphosphino)-2′-(dimethylamino)biphenyl (**L**^{1}) and 2-(dicyclohexylphosphino)-2′-(dimethylamino)-biphenyl (**L**^{2}) have been prepared and structurally characterized by X-ray crystallography. Their dynamic behavior as well as their structural characteristics in solution have been elucidated by the use of NMR techniques. Of particular interest, Pd−N bond rupture occurs with a low barrier (<10 kcal/mol) in the **L**^{1} complex; however, this does not provide a facile pathway for atropisomerization of the ligand. A coordination mode involving η^2 binding of carbon atoms in the (dimethylamino)phenyl moiety was also established for the dicyclohexylphosphino analogue **L**^{2}.

Introduction

The use of chiral nonracemic heterobidentate ligands serves the primary goal of introducing steric as well as electronic asymmetry into a transition-metal complex. Although the rational design of such ligands begins from consideration of monodentate or C_2-symmetric examples, introduction of two different types of donors in a bidentate ligand does not necessarily lead to the anticipated κ^2 coordination mode. Examples of this kind of deviation from expected behavior have been found in complexes of BINAPO,[1] MOP,[2,3] and MAP[2,3] as well as for complexes of the C_2-symmetric ligands BINAP,[4] MeO-BIPHEP,[5,6] NUPHOS,[7] BINOL,[8] and Me$_2$BINOL.[9,10]

Biphenyl analogues[11] of MAP or its partially hydrogenated counterpart H$_8$-MAP,[11] 2-(diphenylphosphino)-2′-(dimethylamino)biphenyl (**L**^{1}), and 2-(dicyclohexylphosphino)-2′-(dimethylamino)biphenyl (**L**^{2}) are axially chiral but have a relatively low barrier to interconversion of the enantiomeric atropisomers (Chart 1).

Chart 1. MAP and Its Atropisomeric Analogues

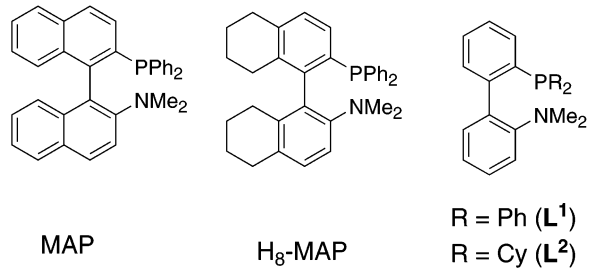

Therefore, one might anticipate that, in contrast to MAP, a racemization pathway would be available for the biphenyl backbones L_1 and L_2 on coordination to a metal, since the hardness of the NMe$_2$ donor would typically render those ligands hemilabile. In particular, a previous[12] report comparing MAP and H$_8$-MAP complexes has shown that H$_8$-MAP prefers the P,N coordination mode. This was attributed to its larger bite angle with respect to MAP. The binaphthyl backbone also provides a beneficial aromatic stabilization in the cases of MAP and MOP. Motivated by the ambiguous NMR data in that report, i.e., the observation of a single resonance for the methyl groups in a given isomer, where the diastereotopicity of the Me groups in each coordinated NMe$_2$ moiety should have given rise to two resonances, we have investigated the behavior of ligands **L**^{1} and **L**^{2}. For complexes of **L**^{1} and **L**^{2} with (allyl)-palladium, we found that the coordination mode depends on the nature of the PR$_2$ group, independent of the presence or absence of a naphthyl backbone.

Results and Discussion

Hemilability in a P,N Complex. The X-ray crystal structure of (η^3-allyl)Pd(L^1)SbF$_6$ (**1**; Figure 1) clearly shows a P,N coordination mode in the solid state that has a single configuration of the allyl relative to the

(1) Cyr, P. W.; Rettig, S. J.; Patrick, B. O.; James, B. R. *Organometallics* **2002**, *21*, 4672−4679.
(2) (a) Kocovsky, P.; Vyskocil, S.; Cisarova, I.; Sejbal, J.; Tislerova, I.; Smrcina, M.; Lloyd-Jones, G. C.; Stephen, S. C.; Butts, C. P.; Murray, M.; Langer, V. *J. Am. Chem. Soc.* **1999**, *121*, 7714−7715. (b) Lloyd-Jones, G. C.; Stephen, S. C.; Murray, M.; Butts, C. P.; Vyskocil, S.; Kocovsky, P. *Chem. Eur. J.* **2000,** *6*, 4348−4357. (c) Kocovsky, P.; Vyskocil, S.; Smrcina, M. *Chem. Rev.* **2003**, *103*, 3213−3245.
(3) Dotta, P.; Kumar, A.; Pregosin, P. S.; Albinati, A.; Rizzato, S. *Organometallics* **2003**, *22*, 5345−5349.
(4) Pathak, D. D.; Adams, H.; Bailey, N. A.; King, P. J.; White, C. *J. Organomet. Chem.* **1994**, *479*, 237−245.
(5) Feiken, N.; Pregosin, P. S.; Trabesinger, G.; Scalone, M. *Organometallics* **1997**, *16*, 537−543.
(6) Feiken, N.; Pregosin, P. S.; Trabesinger, G.; Albinati, A.; Evoli, G. L. *Organometallics* **1997**, *16*, 5756−5762.
(7) Doherty, S.; Newman, C. R.; Hardacre, C.; Nieuwenhuyzen, M.; Knight, J. G. *Organometallics* **2003**, *22*, 1452−1462.
(8) Bergens, S. H.; Leung, P.-H.; Bosnich, B.; Rheingold, A. L. *Organometallics* **1990**, *9*, 2406−2408.
(9) Brunkan, N. M.; White, P. S.; Gagne, M. R. *J. Am. Chem. Soc.* **1998**, *120*, 11002−11003.
(10) Brunkan, N. M.; Gagne, M. R. *Organometallics* **2002**, *21*, 4711−4717.
(11) (a) Tomori, H.; Fox, J. M.; Buchwald, S. L. *J. Org. Chem.* **2000**, *65*, 5334−5341. (b) Shen, X. Q.; Guo, H.; Ding, K. L. *Tetrahedron: Asymmetry* **2000**, *11*, 4321−4327.
(12) Wang, Y.; Li, X.; Sun, J.; Ding, K. *Organometallics* **2003**, *22*, 1856−1862.

10.1021/om030681h CCC: $27.50
Publication on Web 03/31/2004

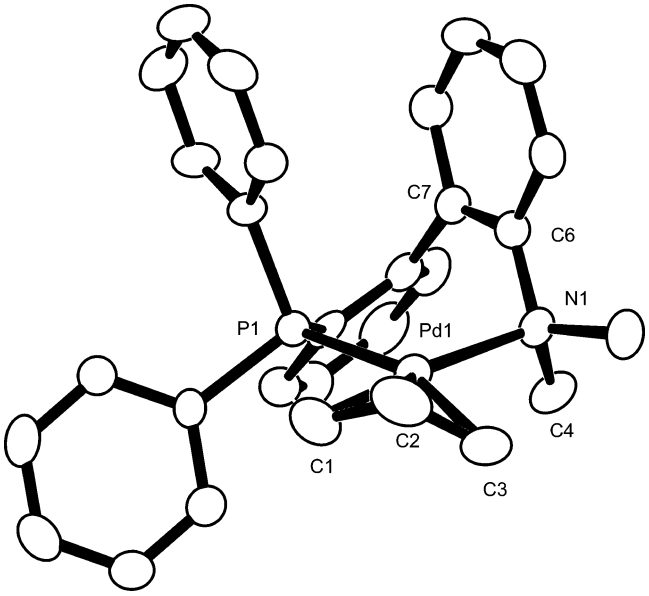

Figure 1. ORTEP diagram of (η^3-allyl)Pd(L^1)SbF_6 (**1**). The crystal is a racemate. The enantiomer shown here has the S,R_{Pd} configuration.

Chart 2. Enantiomers of (allyl)PdXY[a]

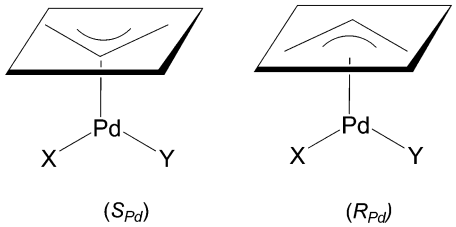

[a] Chirality descriptors assume that the priorities are allyl > X > Y and the centroid of the allyl is out of the plane in the direction of the central carbon.

axial chirality of the ligand. Meso ligands, such as allyl, which are not in the square plane of the palladium produce a potential element of chirality at the palladium. Thus, as shown in Chart 2, there are two enantiomers if no other elements of chirality are present.[13−18]

When yellow crystals of **1** are dissolved in $CDCl_3$ at room temperature, two sets of sharp allyl resonances typical of an η^3-allyl group are observed in a ratio of approximately 1:1. An interesting feature is that there are only two singlet resonances (of relative intensity 6 each) which correspond to the NMe_2 groups of the R^*,R_{Pd}^* and R^*,S_{Pd}^* diastereomers that are present in solution. The diastereotopic nature of the two methyl groups in each of the diastereomers, as inferred from

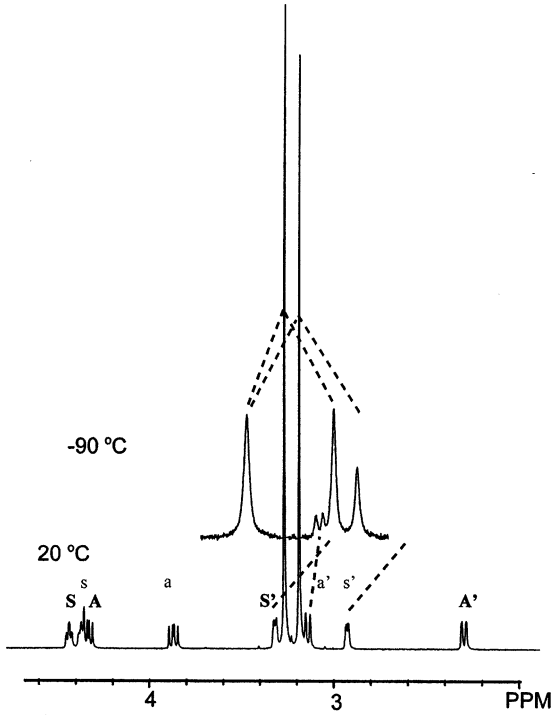

Figure 2. ^{1}H NMR spectrum of an equilibrium mixture of (R^*,R_{Pd}^*)-**1** and (R^*,S_{Pd}^*)-**1**. Syn and anti resonances are noted in upper case for the major isomer (R^*,S_{Pd}^*)-**1**. The 20 °C spectrum was taken in $CDCl_3$, which shows better resolution of resonances at δ ~4.4 than CD_2Cl_2. The −90 °C spectrum was taken in CD_2Cl_2. Note that a terminal allyl resonance, S′, has shifted under the methyl group at δ ~3.0, making its intensity appear anomalously large.

the solid-state structure of **1**, would imply that four singlet resonances (of relative intensity 3 each) should be present. The potential hemilability of ligand $\mathbf{L^1}$ led us to record the low-temperature ^{1}H NMR spectra of **1** in CD_2Cl_2, since a rapid dissociation−reassociation of the NMe_2 group could average the methyl environments. Indeed, at −90 °C, the methyl group resonances of the NMe_2 moieties in both R^*,R_{Pd}^* and R^*,S_{Pd}^* became nonequivalent, as shown in Figure 2, although the two overlap and they were still somewhat broad, owing to the very low barrier associated with this exchange process ($\Delta G^{\ddagger}$ < 10 kcal/mol). We suggest that the coalescence of the methyl resonances of the NMe_2 group arises from Pd−N bond rupture followed by a rapid umbrella inversion at the nitrogen and subsequent bond rotation of the free aryl−NMe_2 prior to reassociation, as shown in Scheme 1.

As the breaking of the Pd−N bond slows at low temperatures, the pathway allowing equilibration of methyl sites is less accessible and decoalescence of the methyl signals occurs. Although the analogue H_8-MAP has been previously investigated by both X-ray crystallography and NMR spectroscopy, the presence of a singlet NMe_2 resonance for each of the exo and endo diastereomers, which are analogous to the R^*,R_{Pd}^* and R^*,S_{Pd}^* forms of **1**, has received little comment.[12] The use of the coalescence of NMe_2 groups to detect hemi-

(13) These isomers are often designated as exo and endo when there is an obvious reference point out of the plane of the square-planar metal moiety.[14,15] This description, however, is ambiguous for a planar PdXY set or in cases where a reference point is not clear. One might view this as a case of planar chirality; however, a nomenclature based on axial chirality was suggested by Hayashi[16] and has been followed by Kocovsky.[2b] This can be awkward when dealing with "axial chirality" of both the ligand and the metal. We have chosen to view the Pd system as one would a chiral pyramidal phosphorus atom, considering the allyl as an 18-electron pseudoatom[17] placed at the centroid of the allyl.[18]

(14) Sprinz, J.; Kiefer, M.; Helmchen, G.; Huttner, G.; Walter, O.; Zsolnai, L.; Reggelin, M. *Tetrahedron Lett.* **1994**, *35*, 1523−1526.

(15) Steinhagen, H.; Reggelin, M.; Helmchen, G. *Angew. Chem., Int. Ed.* **1997**, *36*, 2108−2110.

(16) Hayashi, T.; Kawatsura, M.; Uozumi, Y. *J. Am. Chem. Soc.* **1998**, *120*, 1681−1687.

(17) Sloan, T. E. Stereochemical Nomenclature and Notation in Inorganic Chemistry. *Top. Stereochem.* **1981**, *12*, 1−35.

(18) Faller, J. W.; Stokes-Huby, H. L.; Albrizzio, M. A. *Helv. Chim. Acta* **2001**, *84*, 3031−3042.

Scheme 1. Interconversion of Diastereotopic Methyl Groups

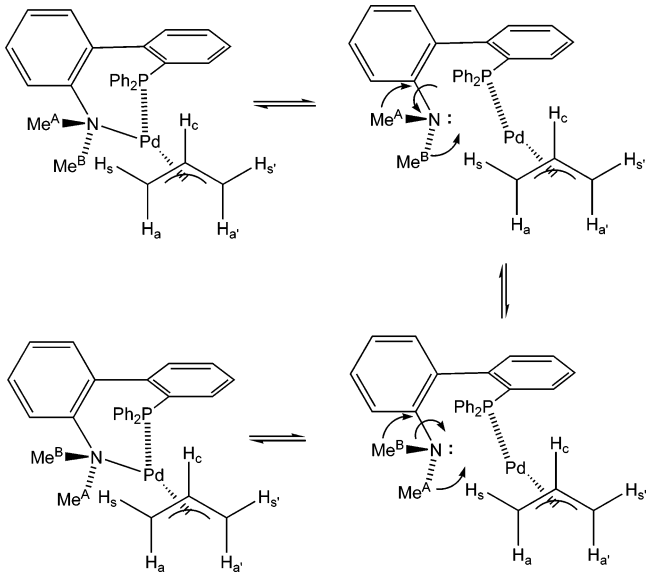

lability, owing to metal−N bond rupture, has been previously investigated by Elguero and co-workers.[19,20] Since the diastereomers of **1** are not interconverted rapidly in this process (vide infra), it appears that there is insufficient time between bond rupture and reformation of the Pd−N bond for atropisomerization to occur at a rapid rate.[21,22]

By dissolution of several crystals of **1** in CD_2Cl_2 at −90 °C and recording of the ^{1}H NMR spectra of the resulting solution as it slowly warmed to −20 °C in the NMR instrument, identification of the allylic resonances corresponding to the R^*,S_{Pd}^* ("crystal") diastereomer was possible. The growth of the second set of allylic resonances that correspond to the R^*,R_{Pd}^* isomer occurred over the course of the experiment, and upon equilibration the ^{1}H NMR of the warmed solution was identical with that obtained by simply dissolving crystals of **1** in CD_2Cl_2 at room temperature. Owing to partial overlap between two resonances of a syn proton, H_s, and an anti proton, H_a, it was difficult to assign those resonances from the ^{1}H NMR spectrum alone. An HMQC spectrum was used for the unambiguous assignments of those resonances. As shown in Figure 2, the resonances for terminal protons trans to the phosphorus (H_s, H_a) are coupled to phosphorus and are at lower field than those that are cis to the phosphorus. Usually resonances for anti protons are upfield of syn protons; however, in the R^*,R_{Pd}^* isomer $H_{s'}$ is at higher field than $H_{a'}$. This could be attributable to the ring current of the biphenyl influencing the anti proton. The time required for epimerization suggested a barrier of between 15 and 20 kcal/mol for the process. This suggested that the process could be observed via line shape or saturation transfer techniques, which could also provide information on the mechanism of epimerization in addition to rate data.

Having established the assignments of the R^*,R_{Pd}^* and R^*,S_{Pd}^* isomers, NMR methods were able to provide information on the details of the mechanism through which the epimerization at the metal center occurred. This was accomplished by performing SST (spin saturation transfer) experiments on the allylic proton resonances at 50 °C, the temperature at which the R^*,S_{Pd}^* proton $H_{a'}$ broadens, owing to exchange ($\Delta G^{\ddagger} = 18.2$ kcal/mol). In particular, it was found that at 50 °C in $CDCl_3$, saturation of the R^*,S_{Pd}^* proton $H_{a'}$ results in the saturation of the R^*,R_{Pd}^* proton $H_{s'}$ while saturation of R^*,S_{Pd}^* H_a resulted in saturation of the R^*,R_{Pd}^* proton H_a. Finally, an EXSY spectrum showed cross-peaks between the $H_{s'}$ and $H_{a'}$ ($H_{a'}$ and $H_{s'}$) resonances as well as cross-peaks between the H_s and H_s (H_a and H_a) resonances of *different* diastereomers. These observations are in accordance with an $\eta^3-\eta^1-\eta^3$ hapticity process of the allyl, where the Pd−C bond trans to the Ph_2P moiety is broken and the palladium F-bonded intermediate allows for epimerization at the metal center (see Scheme 2). This leads, for example, to interconversion of R,S_{Pd} and R,R_{Pd} wherein the chirality in the atropisomeric ligand retains its stereochemistry. The saturation transfer pathway that was found at 50 °C in $CDCl_3$ clearly indicates that epimerization through atropisomerization of the biphenyl-based ligand $\mathbf{L^1}$ is *not* occurring at a significant rate. This ligand epimerization could occur either through a monodentate (P) coordination mode or through a seven-membered-ring inversion. Atropisomerism of the ligand would only involve exchange of anti with anti protons or, alternatively, syn protons with syn protons. One should note that (a) there was not observable saturation

(19) Elguero, J.; Fruchier, A.; de la Hoz, A.; Jalon, F. A.; Manzano, B. R.; Otero, A.; de la Torre, F. G. *Chem. Ber.* **1996**, *129*, 589−594.

(20) Elguero, J.; Guerrero, A.; de la Torre, F. G.; de la Hoz, A.; Jalon, F. A.; Manzano, B. R.; Rodriguez, A. *New J. Chem.* **2001**, *25*, 1050−1060.

(21) The simplest consideration of the intermediate formed upon Pd−N bond rupture is that κ^1P ligand binding is involved. It is possible, however, that there is slippage of the metal to a P,C type of bonding as observed with $\mathbf{L^2}$. Since there is little C=N character in that complex, interconversion of the methyl environments by umbrella inversion could occur via this intermediate, in which the metal would continually be bound to some portion of the dimethylaniline fragment. This would also inhibit atropisomerization in this intermediate.

(22) The barrier for the free ligands $\mathbf{L^1}$ and $\mathbf{L^2}$ have not been reported. The barrier for 2,2′-bis(diphenylphosphino)biphenyl has been reported as 22(1) kcal/mol.[23] The ^{13}C{^{1}H} NMR spectrum of the ligand $\mathbf{L^1}$ at 40 °C in THF-d_8 showed three sharp doublet resonances that correspond to the three ipso carbons at δ 141.0 ($J(P-C_{phenyl}) = 15.7$ Hz), 140.1 ($J(P-C_{phenyl}) = 15.1$ Hz), and 137.7 ($J(P-C_{biphenyl}) = 14.0$ Hz). The ipso carbons in the two phenyls are diastereotopic, owing to slow interconversion of the atropisomers. At 50 °C the resonances at δ 141.0 and 140.1 became broad whereas the resonance at δ 137.7 remained sharp. Since the resonance of the ipso $C_{biphenyl}$ is not expected to broaden with increasing rate of atropisomerization, it was used as an internal standard for the broadness at the given temperature. When the widths of those resonances at half-height ($W_{1/2}$) were compared, it was found that the broadening of the C_{phenyl} resonances was ∼3 Hz at 50 °C. This indicates $\Delta G^* = 17.5$ kcal/mol for the atropisomerization of the free $\mathbf{L^1}$. The protons attached to the α-cyclohexyl carbons in $\mathbf{L^2}$ are diastereotopic at room temperature, indicating a barrier >16 kcal/mol. There are eight carbon atoms in the cyclohexyl groups that are diastereotopic as a consequence of the pyramidal phosphorus; however, the α-carbons directly attached directly to phosphorus as well as the δ carbons are diastereotopic, owing to the axial chirality in the atropisomers, for a total of 12 cyclohexyl ^{13}C resonances. The α-carbon resonances (in THF-d_8 at 50 °C) at δ 39.4 and 36.1 are readily identified, owing to the 17 Hz J_{PC} coupling. These resonances show a small broadening at this temperature, indicating that the barrier is 18.8 kcal/mol. In the ^{1}H spectrum there are 22 diastereotopic protons, of which one attached to an α-carbon appears at δ 2.04, to low field of the others, which are overlapped. This proton is also slightly broadened at 50 °C, owing to exchange. ^{1}H EXSY spectra at this temperature also show 11 cross-peaks, as would be anticipated for atropisomerization—in particular, a cross-peak was observed between protons at δ 2.04 and 1.49, which also correlate with the ^{13}C signals δ 39.4 and 36.1. We were unable to measure the barrier for atropisomerization for the Pd−L^1 complex but presume it would be ∼22 kcal/mol, as found for that with Pd−L^2.

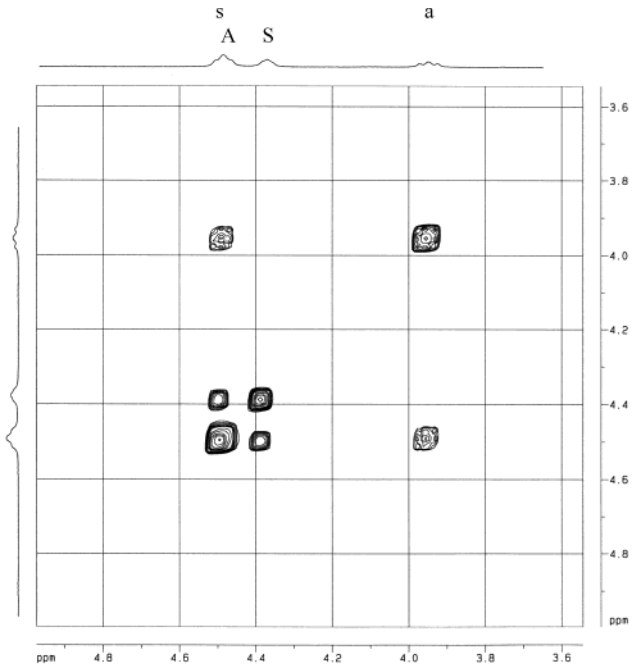

Figure 3. EXSY spectrum of (η^3-allyl)Pd(L^1)SbF_6 (**1**) in $CDCl_3$ at 50 °C, showing the region of the terminal allylic protons trans to the phosphorus atom. Note that the order of some resonances at $\delta \sim 4.4$ has crossed over relative to those observed at 20 °C. The important feature here is that there are no observable cross-peaks between syn and anti protons.

Scheme 2. $\eta^3-\eta^1-\eta^3$ Mechanism Consistent with the Observed Site Exchanges

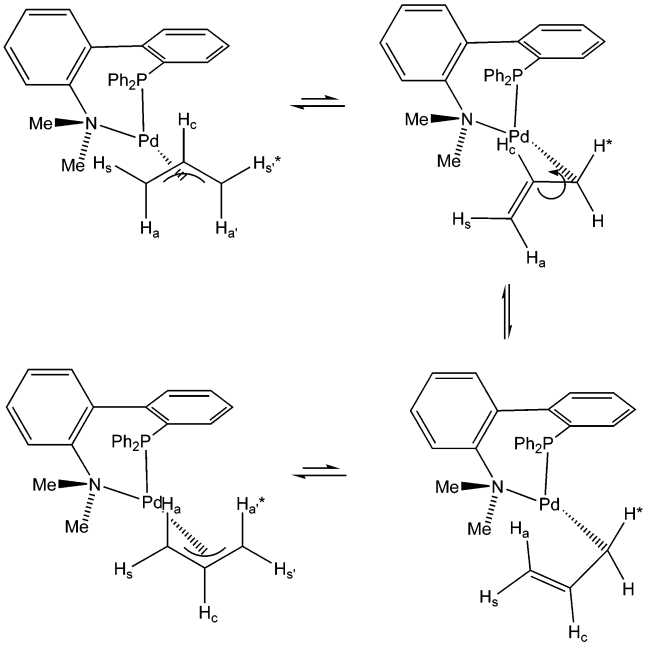

of multiple allylic resonances upon selective saturation of the exo $H_{a'}$ or exo H_a resonances and (b) the EXSY spectrum (Figures 3 and 4) did not show cross-peaks that would suggest such a transformation. This strongly suggests that the absolute configuration of the biphenyl backbone is effectively maintained at room temperature, even though the averaging of the methyl groups of the NMe_2 suggests that the ligand is hemilabile.[21−23]

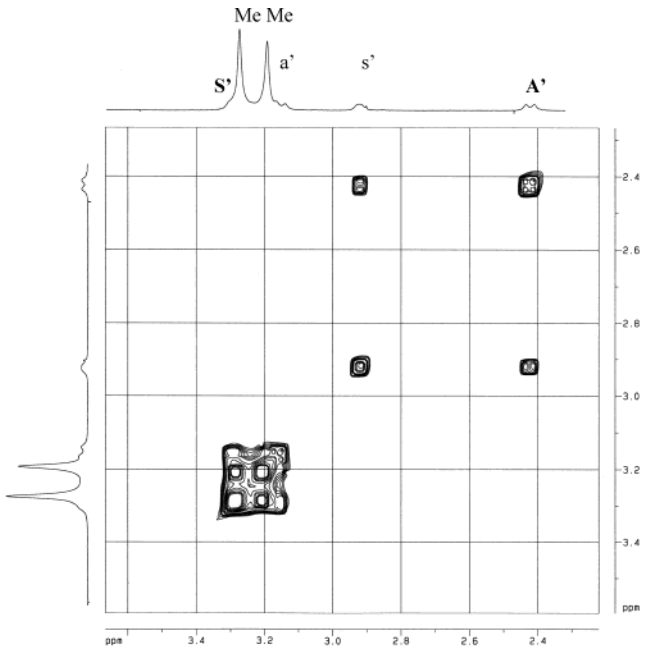

Figure 4. EXSY spectrum of (η^3-allyl)Pd(L^1)SbF_6 (**1**) in $CDCl_3$ at 50 °C, showing the region of the terminal allylic protons cis to the phosphorus atom. The important feature here is that there are observable cross-peaks between syn protons of one diastereomer and anti protons of the other.

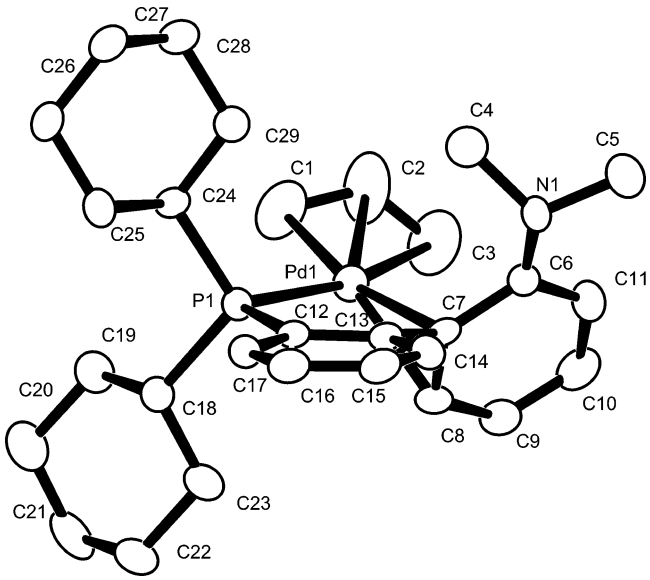

Figure 5. ORTEP diagram of the triclinic (η^3-allyl)Pd(L^2)-SbF_6 (**2**). The crystals contain a racemate. The isomer shown here is S,S_{Pd}.

Novel Binding in (η^3-allyl)Pd(L^2)SbF_6 (2). Crystallographic analysis of the complex (η^3-allyl)Pd(L^2)SbF_6 (**2**) shows not only that $\mathbf{L^2}$ has a different coordination mode than $\mathbf{L^1}$ in **1** but also that crystallization occurs in two different phases, one of which has a chiral space group and may therefore lead to spontaneous resolution. As seen in both crystal forms (Figures 5 and 6), which contain different diastereomers, a P,η^2(C1′−C6′) olefin coordination mode is preferred over the anticipated P,N coordination mode. This contrasts with the known structures of the binaphthyl analogue MAP, which

(23) Desponds, O.; Schlosser, M. *Tetrahedron Lett.* **1996**, *37*, 47−48.

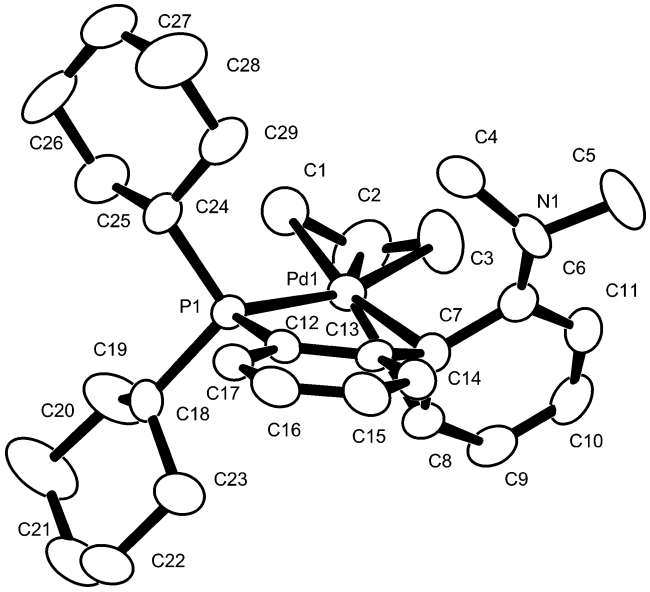

Figure 6. ORTEP diagram of orthorhombic (η^3-allyl)Pd-(L^2)SbF_6 (**2**). A given crystal contains a single enantiomer. The isomer found in this crystal was S,R_{Pd}.

Chart 3. Comparison of Binding in MAP and L^2 [a]

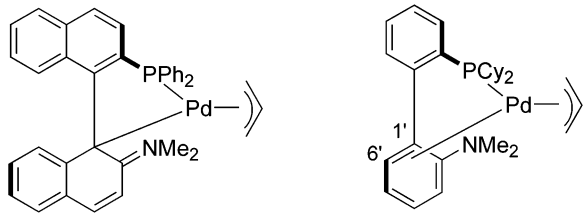

[a] In the $\mathbf{L^2}$ complex the Pd−C1′ and Pd−C6′ bond lengths are 2.441 and 2.330 Å in the triclinic isomer but 2.361 and 2.383 Å in the orthorhombic isomer.

although sometimes bound as a P,C ligand, is generally considered to bind via an η^1 mode[12] (Pd−C = 2.338(11) Å, which is relatively long) (Chart 3).

The NMe_2 group is not planar, and equivalency of the two methyl groups *within the same diastereomer* is anticipated in the ^{1}H NMR spectrum, since the umbrella inversion at the nitrogen atom has a very low barrier, particularly if there is little double-bond character in the N−aryl bond. Indeed, when a CD_2Cl_2 solution of **2** is cooled to −90 °C, only temperature-induced shifting of the two NMe_2 singlet resonances arising from the two diastereomers present was observed in the NMR. This contrasts with the behavior of **1**, which indicates that the NMe_2 group is rapidly dissociating from palladium. An interesting feature of complex **2** is the existence of a relatively large coupling constant ($J_{s'-a'} \approx 2.0$ Hz) between the protons $H_{s'}$ and $H_{a'}$ in both diastereomers. This presumably arises from the fact that the terminal allylic CH_2 allylic moiety trans to the η^2(C1′−C6′) group is more twisted relative to the rest of the allyl fragment. Again, by dissolving a triclinic single crystal at −90 °C in CD_2Cl_2, we were able to observe its isomerization toward the diastereomer present in the orthorhombic crystal, as well as to assign the allylic resonances for each of the isomers.

The metrical parameters for the two isomers can be compared by reference to Table 2. It appears that the P,C binding mode is maintained in solution. Several aspects of the ^{13}C spectrum suggest this, and details for all shifts are included in the Experimental Section. In general, the biphenyl carbons attached to P or N do not show a large coordination shift upon binding of the P or N to the metal. Thus, for **1**, in which $\mathbf{L^1}$ binds in the normal P,N mode, the 2-carbon attached to P shifts from δ 149.0 to δ 149.1 and 148.9, whereas the 2′-carbon attached to N shifts from δ 152.2 to δ 151.9 and 151.8. The double-bond character in the C2′−N bond for $\mathbf{L^2}$ in

Table 1. Crystallographic Data for1 and 2

	1	**2** (triclinic)	**2** (orthorhombic)
color, shape	yellow, needle	yellow, needle	yellow, block
empirical formula	$C_{29}H_{29}F_6NP$-PdSb	$C_{29}H_{41}F_6NP$-PdSb	$C_{29}H_{41}F_6NP$-PdSb
formula wt	764.67	776.76	776.76
radiation, λ/Å	Mo Kα (monochr), 0.710 73		
T/K	173		
cryst syst	monoclinic	triclinic	orthorhombic
space group (No.)	$C2/c$ (15)	$P\bar{1}$ (2)	$P2_12_12_1$ (19)
unit cell dimens			
a/Å	36.8345(4)	11.1900(2)	10.9117(2)
b/Å	9.9269(1)	11.8170(3)	16.5774(3)
c/Å	35.4672(4)	12.4058(3)	17.1390(4)
α/deg	90	98.3213(9)	90
β/deg	115.0758(6)	105.6071(9)	90
γ/deg	90	91.0168(9)	90
V/Å^3	11746.3(2)	1560.56(5)	3100.23(9)
Z	16	4	4
D_{calcd}/g cm^{-3}	1.729	1.653	1.664
μ(Mo Kα)/cm^{-1}	16.43	15.47	15.57
cryst size/mm	0.05 × 0.19 × 0.22	0.10 × 0.14 × 0.19	0.24 × 0.24 × 0.27
total no. of rflns	24 552	12 388	6675
R_{int}	0.045	0.028	0.018
no. of observns ($I > n\sigma(I)$)	7474 ($n = 3$)	4611 ($n = 3$)	3597 ($n = 2$)
no. of params, constraints	739, 0	388, 0	352, 0
R1,[a] wR2,[b] GOF	0.038, 0.037, 1.32	0.039, 0.047, 1.50	0.040, 0.044, 2.22
min, max resid density/e Å^{-3}	−0.73, 1.53	−1.56, 1.24	−1.06, 1.13

[a] $R1 = \sum||F_o| - |F_c||/\sum|F_o|$, for all $I > n\sigma(I)$. [b] $wR2 = [\sum[w(|F_o| - |F_c|)^2]/\sum[w(F_o)^2]]^{1/2}$.

Table 2. Selected Bond Distances (Å)and Angles (deg) for 1 and 2

	1[a]	**2** (triclinic)	**2** (orthorhombic)
	Bond Distances		
Pd1−P1	2.297(1)	2.281(1)	2.289(1)
Pd1−N1	2.211(4)		
Pd1−C1	2.097(5)	2.100(5)	2.126(6)
Pd1−C2	2.163(5)	2.144(6)	2.161(7)
Pd1−C3	2.240(5)	2.235(6)	2.214(6)
Pd1−C7		2.442(5)	2.361(6)
Pd1−C8		2.332(4)	2.383(5)
N1−C4	1.495(6)	1.463(6)	1.455(8)
N1−C5	1.493(6)	1.466(6)	1.468(8)
N1−C6	1.444(6)	1.391(6)	1.355(8)
C1−C2	1.409(7)	1.340(8)	1.42 (1)
C2−C3	1.394(7)	1.332(9)	1.30 (1)
C6−C7	1.410(4)	1.441(6)	1.498(7)
C7−C8	1.405(7)	1.422(6)	1.396(8)
C8−C9	1.377(7)	1.405(6)	1.408(8)
C9−C10	1.366(7)	1.384(7)	1.375(9)
C10−C11	1.364(7)	1.382(7)	1.37 (1)
C11−C6	1.405(7)	1.387(7)	1.388(9)
C7−C13	1.494(7)	1.505(6)	1.493(7)
	Bond Angles		
P1−Pd1−N1	97.9(1)		
P1−Pd1−C7		84.0(1)	84.3(1)
P1−Pd1−C8		93.2(1)	92.9(1)

[a] Distances for only one molecule given.

2, however, leads to a downfield shift of 5.7 or 3.3 ppm (a $\Delta(^{13}C)$ value of 3.6 ppm was observed in the binaphthyl analogue[2]). The largest effects would be expected for the carbon atoms bound to palladium and previously upfield shifts were observed for the binaphthyl analogue,[2] where $\Delta(^{13}C\text{-}1') = -55$ ppm and $\Delta(^{13}C\text{-}6') = -3$ ppm. The binding is primarily to C-1′ in the binaphthyl analogue, whereas there is significant binding to C-6′ in **2**, so that a smaller $\Delta(^{13}C\text{-}1')$ value and a larger $\Delta(^{13}C\text{-}6')$ value would be expected for **2**. The observed coordination shifts for the major and minor isomers of **2** were −26.6 and −22.6 ppm for the carbon $\Delta(^{13}C\text{-}1')$ and −11.6 and −13.6 ppm for $\Delta(^{13}C\text{-}6')$. Therefore, we conclude that the P,C binding mode is maintained in solution.[24]

We were also able to observe the racemization of an orthorhombic single crystal using CD (circular dichroism) spectroscopy. A half-life was observed of approximately 4000 s at 20 °C, which corresponds to a value of $\Delta G^{\ddagger} = 22.5$ kcal/mol. The crystallization of the orthorhombic phase represents a crystallization-induced asymmetric transformation[24] in which one diastereomer is formed as a conglomerate and each crystal should contain only one enantiomer, since the space group is $P2_12_12_1$. In principle, this could provide a method of separating complexes containing the enantiomeric forms of the ligand by manual sorting of the crystals.[26]

In conclusion, we have prepared and characterized two new allyl complexes of palladium which demonstrate that, when a Pd−N bond is present, the ligand is hemilabile and there is a low barrier (<10 kcal/mol) for the Pd−N bond rupture. Nevertheless, a significantly higher barrier (>18 kcal/mol) is required for atropisomerization of the ligand, and diastereomers interconvert via a $\eta^3-\eta^1-\eta^3$ allyl rearrangement. The preference for P,N vs P,C binding is controlled by subtle electronic and steric effects, and P,N bonding is preferred in the Ph_2P case, whereas P,C bonding is preferred in the Cy_2P analogue.

Experimental Section

All reactions were carried out under a nitrogen atmosphere using standard Schlenk techniques. Methylene chloride was distilled over CaH_2. The ligands $\mathbf{L^1}$ and $\mathbf{L^2}$ were purchased from Strem Chemicals. Silver hexafluoroantimonate was purchased from Aldrich Chemicals. The dimers [(η^3-allyl)PdCl] and [(η^3-crotyl)PdCl] were prepared according to a previously published procedure. Standard ^1H and $^{31}P\{^1H\}$ NMR spectra were recorded on Bruker 400 or Bruker 500 and Omega 300 or Omega 500 NMR instruments, respectively. The ^1H VT NMR experiments were performed on an Omega 300 NMR or a Bruker 500 instrument. SST (spin saturation transfer) and EXSY experiments were performed on a Bruker 500 NMR instrument. Elemental analyses were carried out by Atlantic Microlab, Inc., Norcross, GA.

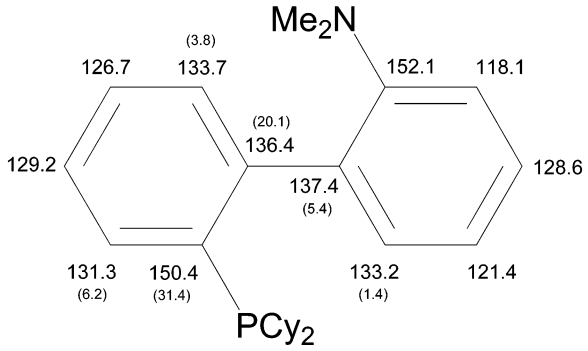

Figure 7. ^{13}C NMR chemical shifts (δ) for $\mathbf{L^2}$ in CD_2Cl_2. $J(^{13}C-^{31}P)$ values are shown in parentheses with accuracies of ±0.2 Hz.

Complexes **1** and **2** were prepared by the same procedures. Typical conditions are as follows for complex **1**.

(η^3-allyl)Pd(L^1)SbF_6 (1). In a flame-dried Schlenk flask, 5 mL of freshly distilled methylene chloride, [(η^3-allyl)PdCl] (11.9 mg, 0.032 mmol), and the ligand $\mathbf{L^1}$ (25 mg, 0.065 mmol) were stirred at room temperature until the solids dissolved completely (∼1 min). Silver hexafluoroantimonate (22.3 mg, 0.065 mmol) was added, and AgCl precipitated almost immediately. The resulting mixture was stirred for an additional $^1/_2$ h and then filtered through Celite. Yellow crystals of analytical purity were obtained in high yield (85%) by slow diffusion of pentane into a methylene chloride solution of the complex. In solution the NMR spectra indicated there was a 53:47 ratio of diastereomers present in CD_2Cl_2.

(a) Crystal Isomer R^*,S_{Pd}^* (Major; Found in a Crystal by VT NMR Starting from −90 °C). ^1H NMR (500 MHz, CD_2Cl_2, δ): 7.67−6.35 (18H, complex, aromatics); 5.89 (1H, m, H_c); 4.37 (1H, br, H_s); 4.33 (1H, dd, H_a, $J_{c-a} = 14.5$ Hz, $J(P-H_a) = 9.0$ Hz); 3.32 (1H, dd, $H_{s'}$, $J_{c-s'} = 6.5$ Hz, $J_{s-s'} = 1.5$ Hz); 3.27 (6H, s, $N(CH_3)_2$); 2.30 (1H, d, $H_{a'}$, $J_{c-a'} = 12.5$ Hz). $^{31}P\{^1H\}$ NMR (202 MHz, $CDCl_3$, δ): 24.1 (s). $^{13}C\{^1H\}$ NMR (125 MHz, CD_2Cl_2, δ, selected resonances): 135−118 (all aromatic C that bear an H showed HMQC cross-peaks in the region); 91.2 (1C, d, $J_{PC} = 25$ Hz, terminal allylic C trans to P); 55.5 (1C, br, terminal allylic C cis to P).

(b) Noncrystal Isomer, R^*,R_{Pd}^* (Minor). ^1H NMR (500 MHz, CD_2Cl_2, δ): 7.67−6.44 (18H, complex, aromatics); 5.89 (1H, m, H_c); 4.44 (1H, br, H_s, partially overlapped with H_a); 3.87 (1H, dd, H_a, $J_{c-a} = 14.0$ Hz, $J(P-H_a) = 10.5$ Hz); 3.19 (6H, s, $N(CH_3)_2$); 3.14 (1H, dd, $H_{a'}$, $J_{c-a'} = 12.0$ Hz); 2.93 (1H, d, $H_{s'}$, $J_{c-s'} = 6.5$ Hz, $J_{s-s'} = 2.0$ Hz). $^{31}P\{^1H\}$ NMR (202 MHz, $CDCl_3$, δ): 22.7 (s). $^{13}C\{^1H\}$ NMR (125 MHz, CD_2Cl_2, δ, selected resonances): 135−118 (all aromatic C that bear an H showed HMQC cross-peaks in the region); 87.9 (1C, d, $J_{PC} = 25$ Hz terminal allylic C trans to P); 60.1 (1C, br, terminal allylic C cis to P). Anal. Calcd for $C_{29}H_{29}NF_6PPdSb$: C, 45.55; H, 3.82; N, 1.83. Found: C, 45.63; H, 3.75; N, 1.83.

(η^3-allyl)Pd(L^2)SbF_6 (2). Assignments were made with the assistance of J values, HMQC, and COSY. In solution the NMR spectra indicated there was a 58:42 ratio of diastereomers present at equilibrium in CD_2Cl_2. Comparisons of ^{13}C shifts are most easily followed by reference to Figures 7 and 8.

(a) R^*,S_{Pd}^*, the Major Isomer at Equilibrium. This is the isomer found in the orthorhombic crystals. These resonances did not appear after triclinic crystals were dissolved

(24) We have assumed that the type of binding found in the solid persists in solution. The much lower barrier for methyl interconversion for the NMe_2 group in **2** relative to that in **1** also supports this assumption. There are also (1) shifts of anti protons to lower field than syn protons and (2) protons cis to phosphine that are to lower field than those trans to phosphine, which are not normally observed.

(25) Vedejs, E.; Donde, Y. *J. Org. Chem.* **2000**, *65*, 2337−2343.

(26) We have found resolutions of this type useful in a number of cases, but this one is not ideal. The formation as a triclinic or orthorhombic phase is random, although it appears that seeding can induce one form. A more critical problem is that the orthorhombic crystals have a propensity for forming racemic twins. Thus, a given crystal will have a nonracemic mixture, but the fraction can vary. For example, a large orthorhombic crystal was cut and the larger portion of the crystal was used for a planned CD experiment; however, the remaining portion which was used for X-ray analysis was a ∼55:45 racemic twin and the crystal showed a very weak dichroism, indicating a nearly racemic mixture. Testing several large crystals by CD gave results which indicated that racemic twinning was common; however, in some crystals the twinning was minimal and the CD could be determined and used as a diagnostic for racemization rate. We are still investigating these phenomena.

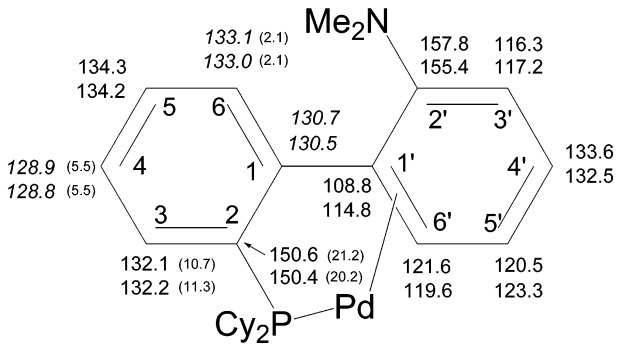

Figure 8. ^{13}C NMR chemical shifts (δ) for (η^3-allyl)Pd(L^2)SbF_6 (**2**) in CD_2Cl_2. $J(^{13}C-^{31}P)$ values are shown in parentheses with accuracies of ±0.2 Hz. The upper shifts are for the major isomer. Shifts in italics are tentative, owing to overlap in the HMQC spectra.

in CD_2Cl_2 at low temperature but were observed after the solution was warmed to room temperature.

^1H NMR (400 MHz, CD_2Cl_2, δ): 7.78−6.62 (8H, complex, aromatics); 5.51 (1H, m, H_c); 4.05 (1H, ddd, $H_{s'}$, $J_{c-s'} = 6.4$ Hz, $J_{s-s'}$. $J_{s'-a'}$. 2.0 Hz); 3.97 (1H, dd, H_a, $J_{c-a} = 14.0$ Hz, $J(P-H_a) = 8.0$ Hz); 2.90 (6H, s, $N(CH_3)_2$); 2.71 (2H, H_s and $H_{a'}$ overlapped). $^{31}P\{^1H\}$ NMR (122 MHz, CD_2Cl_2, δ): 46.9 (s). $^{13}C\{^1H\}$ NMR (125 MHz, CD_2Cl_2, δ, selected resonances): 135−115 (all aromatic C that bear an H showed HMQC cross-peaks in the region); 119.6 (1C, d, $J_{PC} = 6$ Hz, central allylic C); 100.5 (1C, d, $J_{PC} = 27$ Hz, terminal allylic C trans to P); 55.5 (1C, s, terminal allylic C cis to P); 37.9 (1C, d, cyclohexyl P-*C*-H, $J_{CP} = 24$ Hz); 37.4 (1C, d, cyclohexyl P-*C*-H, $J_{CP} = 24$ Hz).

A difference NOE showed that irradiation of *Me*−N at δ 2.90 enhanced a doublet at δ 7.11, indicating that it should be assigned to the 3′-proton. This implied that the remaining upfield doublet at δ 6.62 was the 6′-proton. COSY data allowed assignments of the protons in the rings, assuming the largest J_{PH} value was to H-3. HMQC data then allowed the carbon assignments shown in Figure 8. ^{13}C data for carbon atoms not bearing a proton were relatively weak, particularly the resonance at δ 155.4, but positions were verified with HMQC data optimized for long-range couplings.

(b) Minor Isomer (Found in a Triclinic Crystal by VT NMR Starting from −90 °C). ^1H NMR (400 MHz, CD_2Cl_2, δ): 7.78−6.79 (8H, complex, aromatics); 5.51 (1H, m, H_c); 3.91 (1H, ddd, $H_{s'}$, $J_{c-s'} = 6.8$ Hz, $J_{s-s'}$. ≈ $J_{s'-a'}$ ≈ 2.2 Hz); 3.56 (1H, dd, H_a, $J_{c-a} = 13.6$ Hz, $J(P-H_a) = 8.8$ Hz); 3.22 (1H, ddd, H_s, $J_{c-s} \approx J(P-H_s) \approx 8.4$ Hz, $J_{s-s'} \approx 2.2$ Hz); 2.93 (1H, d (br), $H_{a'}$, $J_{c-a'} = 12.8$ Hz); 2.81 (6H, s, $N(CH_3)_2$). $^{31}P\{^1H\}$ NMR (122 MHz, CD_2Cl_2, δ): 43.1 (s). $^{13}C\{^1H\}$ NMR (125 MHz, CD_2Cl_2, δ, selected resonances): 135−115 (all aromatic C that bear an H showed HMQC cross-peaks in the region); 119.9 (1C, d, $J_{PC} = 6$ Hz, central allylic C); 96.4 (1C, d, $J_{PC} = 27$ Hz, terminal allylic C trans to P); 53.5 (1C, s, terminal allylic C cis to P); 38.0 (1C, d, cyclohexyl P−*C*−H, $J_{CP} = 24$ Hz); 37.0 (1C, d, cyclohexyl P−*C*−H, $J_{CP} = 24$ Hz). Anal. Calcd for $C_{29}H_{41}NF_6PPdSb$: C, 44.84; H, 5.32; N, 1.80. Found: C, 44.59; H, 5.26; N, 1.93.

Structure Determination and Refinement. Crystals were obtained by slow diffusion of pentane into methylene chloride solution of complexes **1** and **2**. Data were collected on a Nonius KappaCCD (Mo Kα radiation) diffractometer and were not specifically corrected for absorption, other than the inherent corrections provided by Scalepack.[27] The structures were solved by direct methods (SIR92)[28] and refined on *F* for all reflections.[29] Non-hydrogen atoms were refined with anisotropic displacement parameters. Hydrogen atoms were included at calculated positions. Relevant crystal and data parameters are presented in Table 1.

Structure Determination of 1. This structure determination was straightforward, and the compound had crystallized in a monoclinic cell with $Z = 16$, indicating a space group of *C*2/*c*, which requires two molecules in the asymmetric unit. The molecules are nearly identical, and only one is shown in Figure 1.

Structure Determination of Triclinic 2. This structure determination was straightforward, and the compound had crystallized in a triclinic cell with $Z = 2$, indicating a space group of $P\bar{1}$.

Different crystallization vials tended to contain an excess of either triclinic or orthorhombic crystals, suggesting a seeding phenomenon. SbF_6 showed a 2:1 disorder, which was modeled as a rotation about one F−Sb−F axis of ∼45°.

Structure Determination of Orthorhombic 2. The data showed an orthorhombic cell with absences consistent with the space group $P2_12_12_1$. The Flack parameter was ambiguous, and the opposite hands were refined with only a minor difference in *R* factors (*R*, R_w, GOF of 4.08, 4.61, 2.31 vs 3.99, 4.43, 2.22). Refinement with SHELX suggested a racemic twin with a ratio of ∼45:55. The enantiomer shown in the ORTEP diagram gave the lowest *R* factor on refinement on *F*.

Acknowledgment. This work was supported by the National Science Foundation (Grant No. CHE0092222).

Supporting Information Available: Listings of atomic positions, thermal parameters, and bond distances and angles for **1** and **2**. This material is available free of charge via the Internet at http://pubs.acs.org.

OM030681H

(27) HKL2000 (Denzo-SMN) software package: Minor, W.; Otwinowski, Z. Processing of X-ray Diffraction Data Collected in Oscillation Mode. In *Methods in Enzymology*; Carter, C. W., Jr., Sweet, R. M., Eds.; Academic Press: New York, 1997; Vol. 276A (Macromolecular Crystallography), pp 307−326.

(28) Altomare, A.; Cascarano, G.; Giacovazzo, C.; Guagliardi, A. *J. Appl. Crystallogr.* **1993**, *26*, 343.

(29) TEXSAN for Windows version 1.06: Crystal Structure Analysis Package; Molecular Structure Corp., The Woodlands, TX, 1997−1999.